

TTS-1 Technical Report



Abstract

We introduce Inworld TTS-1, a set of two Transformer-based autoregressive text-to-speech (TTS) models. Our largest model, **TTS-1-Max**, has 8.8B parameters and is designed for utmost quality and expressiveness in demanding applications. **TTS-1** is our most efficient model, with 1.6B parameters, built for real-time speech synthesis and on-device use cases. By scaling train-time compute and applying a sequential process of pre-training, fine-tuning, and RL-alignment of the speech-language model (SpeechLM) component, both models achieve state-of-the-art performance on a variety of benchmarks, demonstrating exceptional quality relying purely on in-context learning of the speaker’s voice. Inworld TTS-1 and TTS-1-Max can generate high-resolution 48 kHz speech with low latency, and support 11 languages with fine-grained emotional control and non-verbal vocalizations through audio markups. We additionally open-source our training and modeling code under an MIT license.

Code: <https://github.com/inworld-ai/tts>

Examples: <https://inworld-ai.github.io/tts>

Playground: <https://inworld.ai/tts>

1 Introduction

Recent advancements in deep learning and the proliferation of large-scale audio datasets [1–3] have propelled text-to-speech (TTS) synthesis from multi-stage pipelines [4, 5] to end-to-end generative systems [6–8]. The latest paradigm leverages large language models (LLMs) [9, 10] as powerful speech-language models (SpeechLMs), using neural audio codecs as tokenizers to generate highly naturalistic speech from text [11–15]. Despite this progress, many existing models struggle to meet the demands of real-world applications, often lacking high-fidelity output (e.g., 48 kHz), robust multilingual support, reliable real-time streaming capabilities, or suffering from synthesis artifacts.

This paper introduces Inworld TTS-1 and TTS-1-Max, two generative speech models designed to bridge this gap. Our models, based on 1B and 8B parameter LLaMA backbones respectively, achieve state-of-the-art speech quality and control through a systematic training methodology and architectural innovations. We demonstrate that a sequential process of pre-training, supervised fine-tuning (SFT), and reinforcement learning (RL) alignment is critical for developing high-performance TTS systems. Our key contributions are as follows:

- **A three-stage training framework for SpeechLMs.** We propose a robust pipeline consisting of (1) large-scale pre-training on over 1M hours of raw audio mixed with text data [16, 17] to build a strong foundational model; (2) supervised fine-tuning on 200k hours of high-quality, filtered audio-text pairs; and (3) reinforcement learning alignment using Group Relative Policy Optimization (GRPO) [18] to fine-tune the model against perceptual quality metrics and reduce hallucinations.
- **A high-resolution audio codec for 48 kHz speech synthesis.** We develop a novel audio codec built on top of the X-codec2 [19] architecture with a super-resolution module to natively generate 48 kHz audio. We introduce an root mean-square (RMS) loudness loss term during training to ensure volume consistency, a critical factor for streaming applications.
- **An extensible reinforcement learning framework for speech quality.** We adapt GRPO for TTS alignment. We design a composite reward function combining word error rate (WER), speaker similarity (SIM) [20], and DNSMOS scores [21]. The framework is modular, allowing for the integration of further reward signals like prosody or emotion consistency.
- **Expressive and controllable speech synthesis.** We enable fine-grained control over non-verbal vocalizations and speaking styles through textual *audio markups*. We show that pairing neutral and

stylized utterances from the same speaker during a LoRA-based [22] fine-tuning phase is an effective strategy for teaching the model stylistic control while preserving speaker identity.

- **Efficient and robust streaming inference.** We detail a low-latency streaming pipeline that employs novel techniques, including context-aware decoding and concatenation at non-voicing regions, to ensure seamless and high-quality audio delivery in real-time scenarios.

Our models generate high-fidelity 48 kHz speech, support 11 languages, and offer fine-grained emotional control through in-context learning from short reference audio clips. Through extensive evaluations, we demonstrate their superior performance and practical utility for a wide range of applications, from interactive assistants to content creation. To facilitate further research and development in the community, we open-source our training, modeling, and benchmarking code under a permissive license.

2 Architecture

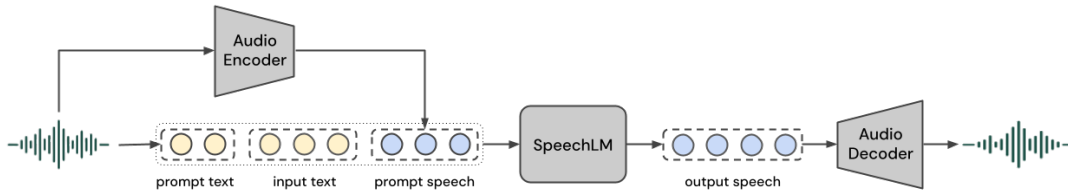


Figure 1. The architecture of Inworld TTS-1. The audio encoder tokenizes a reference audio into a sequence of discrete audio tokens. These tokens are concatenated with the tokenized reference text and the text to be synthesized to form a prompt for the SpeechLM. The SpeechLM autoregressively generates audio tokens, which are then converted back into a 48 kHz waveform by the audio decoder.

Inworld TTS-1 and TTS-1-Max are built on the same architecture as shown in Figure 1: they use the same audio encoder and decoder components and only differ in the size of the SpeechLM backbone used. With all inference components combined, the models have 1.6B and 8.8B parameters, respectively. Below we outline key aspects of both components.

2.1 Audio Codec

Audio codec selection plays a critical role in building a high-quality TTS model. We opted for the codec architecture of X-codec2 [19], which merges both acoustic and semantic information of the encoded audio into a single codebook of 65536 tokens and generates 50 tokens per second of audio.

The selection of this codec architecture was motivated by several key factors:

- **Streaming inference.** The architectural simplicity and 1D causal structure of the audio tokens enable efficient streaming inference with minimal communication overhead.
- **Open-source implementation.** The availability of source code facilitated training the codec from scratch on large-scale datasets and enabled adaptation for high-resolution audio processing (the original implementation was limited to 16 kHz audio).
- **Computational efficiency.** The compact one-dimensional codebook structure enables efficient storage and processing of tokenized audio data. For instance, encoding 1 hour of raw 48 kHz mono audio requires ~ 365 MB of storage, while the tokenized representation from a codebook of 65536 tokens requires only ~ 0.19 MB using uint16 data types.

To support high-resolution speech synthesis, we augmented the original X-codec2 decoder with a super-resolution module. The baseline X-codec2 decoder architecture employs a backbone model comprising ResNet blocks [23] and transformer layers to predict acoustic features from audio tokens. These predicted acoustic features are subsequently converted to an audio waveform via an inverse short-time Fourier transform (iSTFT).

The temporal resolution of the generated audio is determined by two factors: the resolution of the predicted acoustic features and the hop length parameter of the iSTFT operator. In the original implementation, for one second of audio, the decoder’s backbone model processes 50 input tokens and applies iSTFT with a hop

length of 320 samples, yielding 16 kHz audio output. Our super-resolution module extends this architecture through interleaved strided 1D transposed convolutional layers and ResNet blocks. The transposed convolution layers increase the temporal resolution of predicted acoustic features by predetermined stride factors. When combined with appropriately adjusted iSTFT hop lengths, this module enables audio generation with higher sample rates while introducing minimal computational overhead.

Table 1 provides comprehensive details regarding the stride configurations and corresponding iSTFT hop lengths employed in our implementation.

Component	Sample Rate	Strides	Hop length	Parameter Count, M
Audio Encoder	16 kHz	N/A	320	55.28
Audio Decoder	16 kHz	1	320	187.00
Audio Decoder	24 kHz	1	480	187.65
Audio Decoder	48 kHz	3, 2	160	193.43

Table 1. Trainable parameter counts for the audio encoder and decoder.

Notably, our proposed decoder uses a significantly larger hop length compared to other iSTFT-based audio generation models. For example, Du et al. [15] use a hop length of 4 for 24 kHz audio generation, while we empirically found that for 48 kHz audio generation our model yields better speech quality.

2.2 SpeechLM

TTS-1 and TTS-1-Max employ LLaMA-3.2-1B and LLaMA-3.1-8B [24] as their respective SpeechLM backbones. The vocabulary of each model was expanded from 128256 to 193856 tokens, incorporating 65536 audio tokens and 29 special tokens. The resulting vocabulary size was padded to be a multiple of 32 for computational efficiency [25]. Notably, a vocabulary size of 193800 was used during an intermediate pre-training phase before the final requirements for instruction-following were established.

The embeddings for new vocabulary tokens were initialized by sampling from a multivariate normal distribution with the mean and covariance of the original embedding matrix [26].

3 Training Methodology

3.1 Data

The training corpus for our models comprises a large-scale, multilingual audio-text dataset curated from a combination of publicly available sources and licensed third-party providers. This corpus is partitioned into two main subsets for pre-training and supervised fine-tuning, respectively.

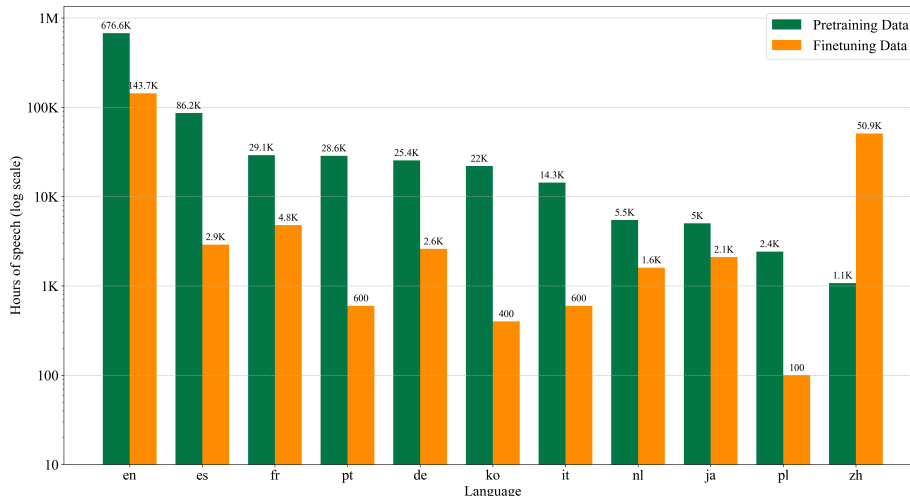


Figure 2. Speech data quantities per language and dataset.

Pre-training. The pre-training dataset contains ~ 1 million hours of raw audio. To enhance model robustness against diverse, real-world acoustic environments, this set is augmented with ~ 30000 hours of non-speech audio, including environmental sounds, background noise, and multi-speaker babble. The linguistic composition of the speech portion is detailed in Figure 2. Additionally, an initial ~ 15000 -hour high-quality subset from our fine-tuning data was incorporated into the pre-training mixture to bootstrap the model’s text-to-speech alignment capabilities.

Fine-tuning. The supervised fine-tuning (SFT) dataset consists of ~ 200000 hours of high-quality, transcribed audio-text pairs. This data was carefully filtered and prepared for subsequent training stages. Further details on data processing and annotation for specific training phases are provided in the corresponding sections.

3.2 Audio Codec

We follow the same methods as X-codec2 [19] to train the audio codec. The only notable difference is how we trained the audio decoder component, which we describe in more detail below.

Experiments. We train our audio codec on about 110k hours of multilingual audio data sourced from both pre-training and fine-tuning datasets described in Section 3.1. In early experiments, we observed that the decoder’s output often failed to preserve the perceived volume of the original audio, especially when decoding short or high-pitched segments. As a consequence, when these segments are concatenated during streaming, the user may perceive sudden increases or drops in volume.

To address this, we introduced an additional root mean-square (RMS) loudness loss term that penalizes discrepancies in volume between the original and decoded waveforms. RMS is a standard statistical measure used to approximate perceived loudness, making it a natural choice for enforcing consistency. The training loss is defined similarly to Xin et al. [27]:

$$\mathcal{L}_{decoder} = \lambda_{disc} \cdot \mathcal{L}_{disc} + \mathcal{L}_{gen} + \lambda_{RMS} \cdot \mathcal{L}_{RMS} \quad (1)$$

$$\mathcal{L}_{gen} = \lambda_{adv} \cdot \mathcal{L}_{adv} + \lambda_{fm} \cdot \mathcal{L}_{fm} + \lambda_{mel} \cdot \mathcal{L}_{mel} \quad (2)$$

where \mathcal{L}_{disc} is the discriminator loss derived from the multi-period discriminator (MPD) [28] and the multi-scale STFT discriminator (MSD) [19, 29]; \mathcal{L}_{gen} is the generator loss, which includes the mel spectrogram loss, feature matching loss, and the adversarial loss [28]. The new \mathcal{L}_{RMS} term is defined as:

$$\mathcal{L}_{RMS} = \mathbb{E} \left[X_t - \hat{X}_t \right]^2 \quad (3)$$

$$X_t = 20 \log_{10} \left(\sqrt{\frac{1}{T} \sum_{t=1}^T x_t^2 + \epsilon} \right) \quad (4)$$

where X_t and \hat{X}_t are the original and generated audio samples volumes in decibels, T is the corresponding waveform array length, and $\epsilon = 10^{-5}$ is a small constant for numerical stability. In our experiments we found that $\lambda_{RMS} = 1.0$ works well for both 24 kHz and 48 kHz audio.

To achieve 48 kHz audio synthesis, up-training was performed in two stages: first with audio samples having sample rates ≥ 32 kHz, then with additional fine-tuning on audio with native sample rates ≥ 44.1 kHz. This progressive training strategy ensures robust high-fidelity audio generation across varied scenarios.

Evaluation results. Subjective evaluation reveals that the 48 kHz decoder produces clearer audio with richer high-frequency details. This finding is consistent with the DNSMOS scores presented in Table 2, where the 48 kHz decoder achieves the highest audio quality.

Sample Rate	DNSMOS
16 kHz	4.110
24 kHz	4.178
48 kHz	4.195

Table 2. DNSMOS scores for decoder models trained with different sample rates. The evaluation is performed on the English subset of the Seed-TTS evaluation [13].

3.3 SpeechLM Pre-Training

To enable the model to precisely recreate an arbitrary speaker’s voice, encompass a wide range of pitch variations, and reproduce non-verbal vocalizations, the model was pre-trained on a diverse corpus of authentic speech.

Experiment setup. The raw audio data underwent minimal processing and was segmented into samples with a maximum duration of 40 seconds, a constraint imposed by the audio encoder’s architecture. Each sample was demarcated by `<|speech_start|>` and `<|speech_end|>` special tokens to facilitate the model’s ability to learn continuous speech patterns.

The audio data was supplemented with approximately 10% text data from the RedPajama-v2 pre-training dataset [16], which was filtered using simple heuristics to retain high-quality, long-form documents. Also, following the findings of [30], we added instruction data from LAION OIG [17] as raw text tokens to the text dataset to help the model’s ability to understand text. Overall, around 20B text tokens were used for both models’ pre-training. This approach was observed to prevent the degradation of text comprehension abilities during subsequent supervised fine-tuning stages, without adversely affecting speech synthesis quality.

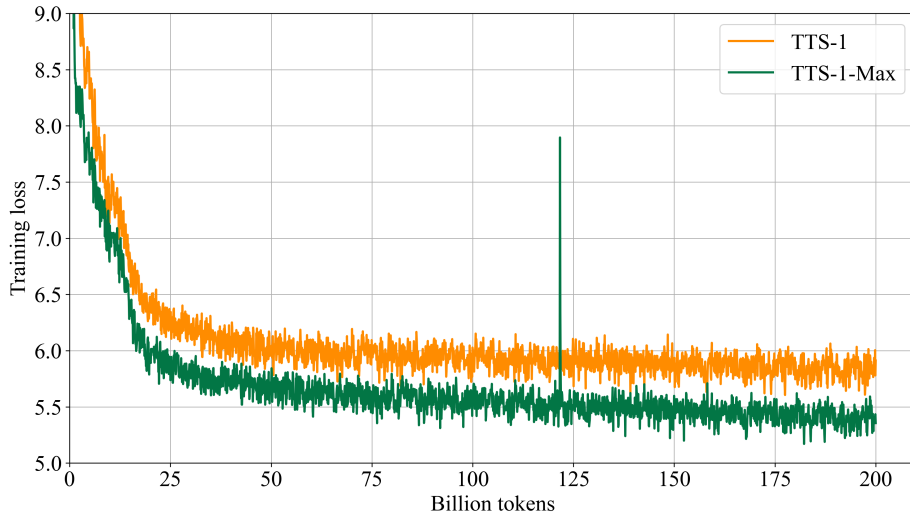


Figure 3. Pre-training loss for the TTS-1 and TTS-1-Max SpeechLM models.

For training we use a standard technique to perform unsupervised language modeling via next token prediction [31] using the hyperparameters shown in Table 3.

Hyperparameter	TTS-1	TTS-1-Max
Training strategy	DDP	FSDP
Per-GPU batch size	8	2
Gradient accumulation steps	1	4
Total number of GPUs		32
Maximum sequence length		2048
Optimizer	AdamW, $\beta_1 = 0.9$, $\beta_2 = 0.95$	
Learning rate (peak)	1.5×10^{-4}	
Learning rate schedule	Cosine decay (10% warmup)	
Weight decay	0.1	

Table 3. Pre-training hyperparameters for TTS-1 and TTS-1-Max.

To optimize training throughput, we employed a combination of bf16 mixed-precision training, FlashAttention-2 [32], and the fused AdamW optimizer [33]. For distributed training, the Distributed Data Parallel (DDP) strategy [34] was applied to the smaller TTS-1 model. For the larger TTS-1-Max model, we adopted the Fully Sharded Data Parallel (FSDP) strategy [35] to maximize GPU utilization. Additionally, given the fixed sequence length of any given batch during pre-training we used `torch.compile()` to further optimize the training throughput.

On average we were able to achieve ~ 46000 and ~ 8000 tokens/sec/GPU for TTS-1 and TTS-1-Max respectively using 32 H100 GPU with 80GB of memory. Single pre-training run for TTS-1 and TTS-1-Max took ~ 2 and ~ 10 days respectively.

Evaluation results. The performance of the pre-trained TTS-1 and TTS-1-Max models is benchmarked on a multi-lingual test set of approximately 5,000 utterances with an average duration of 10 seconds. Voice similarity is quantified as the cosine similarity (SIM) between speaker embeddings from the generated and reference audio, extracted using a WavLM-large model fine-tuned for speaker verification [20]. For our evaluation, each utterance is bisected: the first half serves as the reference audio prompt for the model to generate the subsequent half, which is then compared against the ground truth. Speech is synthesized by decoding the raw token distribution with $top_k = 50$, $top_p = 1.0$ and $T = 1.0$.

The results, presented in Figure 4, indicate that the overall performance correlates with the training loss difference between both models that is depicted in Figure 3. Notably, the improvements in prompt continuation similarity are more pronounced for the larger TTS-1-Max model compared to TTS-1.

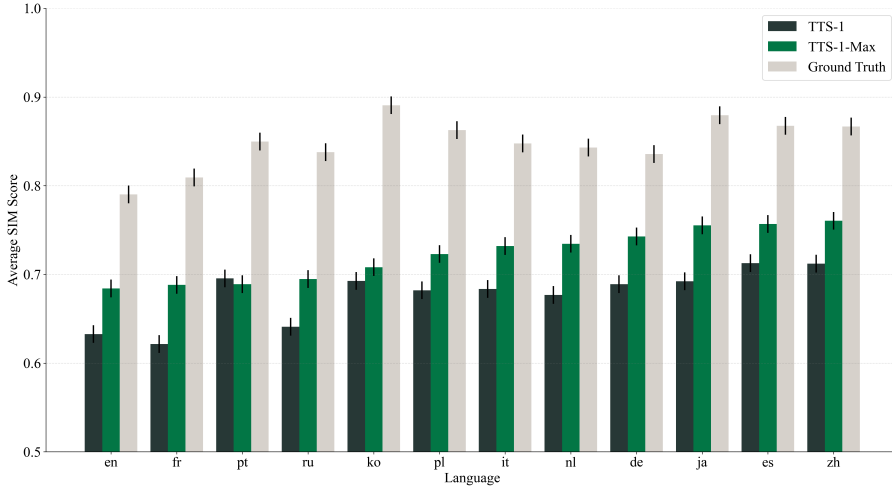


Figure 4. Performance of TTS-1 and TTS-1-Max pre-trained SpeechLM checkpoints on the test set. Cross-language results are not directly comparable as each language subset contains distinct utterances.

3.4 SpeechLM Supervised Fine-Tuning

For supervised fine-tuning (SFT), we adopt a standard autoregressive training objective, consistent with prior work in speech synthesis [13–15, 19]. The model is trained to predict each audio token conditioned on the input text prompt and the preceding ground-truth audio tokens. This is achieved by minimizing the negative log-likelihood of the target sequence, defined as:

$$\mathcal{L}_{\text{SFT}} = - \sum_{s=1}^S \log P(y_s | x_1, \dots, x_T, y_1, \dots, y_{s-1}) \quad (5)$$

where $\{x_1, \dots, x_T\}$ represents the sequence of input text tokens and $\{y_1, \dots, y_S\}$ is the sequence of target audio tokens. During the training the input sequence is constructed as follows:

$$\langle \text{<|begin_of_text|>, } x_1, \dots, x_T, \text{<|speech_start|>, } y_1, \dots, y_S, \text{<|speech_end|>} \rangle \quad (6)$$

Experiment setup. To enhance the quality of the generated speech, the audio data was systematically pre-processed. We annotated the dataset with DNSMOS scores [21] to quantify audio quality and measured characters per second (CPS) to determine talking speed. A multi-stage filtering process was then applied. Inspired by [36], we first discarded the 20% of samples with the lowest DNSMOS scores, which correspond to the low-quality tail of the distribution. Next, we computed language-specific CPS distributions and filtered out the fastest 5% and slowest 5% of samples, as these outliers often contain malformed audio or transcription errors. Finally, we applied text-based heuristics to remove samples with low-quality transcriptions, such as

those containing only punctuation, or other non-speech content. This filtering pipeline yielded a final dataset of approximately 200000 hours of high-quality audio.

As an initial checkpoint for both TTS-1 and TTS-1-Max, we used the audio pre-trained SpeechLM checkpoints from the previous stage (Section 3.3). We found that initializing the SFT learning rate to the final learning rate from pre-training was crucial for achieving optimal speech quality. The other hyperparameters for SFT are detailed in Table 4.

Hyperparameter	TTS-1	TTS-1-Max
Training strategy	DDP	Deepspeed Stage 2
Per-GPU batch size	4	2
Gradient accumulation steps	1	2
Total number of GPUs		32
Maximum sequence length		2048
Optimizer	AdamW, $\beta_1 = 0.9$, $\beta_2 = 0.95$	
Learning rate (peak)	1.5×10^{-5}	
Learning rate schedule	Cosine decay (5% warmup)	
Weight decay	0.1	

Table 4. SFT hyperparameters for TTS-1 and TTS-1-Max.

Throughout the SFT training, the audio codec was loaded on each GPU to periodically perform inference to generate audio samples for quality evaluations. This imposed an additional memory overhead of ~ 4 GB per GPU; therefore, the FSDP setup requiring more memory for a larger model was replaced with Deepspeed Stage 2 [37]. Also, given the variable maximum sequence length of any given batch during SFT, `torch.compile()` was not applicable, and the final training throughput was approximately ~ 18000 and ~ 4800 tokens/sec/GPU for TTS-1 and TTS-1-Max, respectively, using the same training cluster as for pre-training.

Challenges with mixed-objective fine-tuning. We investigated the effect of incorporating text-based instruction-following data during SFT to improve the model’s interpretation of nuanced prompts. However, this approach led to a notable degradation in synthesis quality, with the model often failing to generate speech reliably. This occurred despite observing no adverse impact on the training loss for the audio portion of the mixed dataset.

Impact of pre-training. The use of a pre-trained SpeechLM as the starting point for SFT proved to be crucial for achieving high-quality results. As shown in Figure 5, an ablation study on a 100k-hour multilingual data subset demonstrates that fine-tuning from an audio pre-trained checkpoint yields a lower training loss compared to starting from the base LLaMA-3.2-1B-Instruct checkpoint.

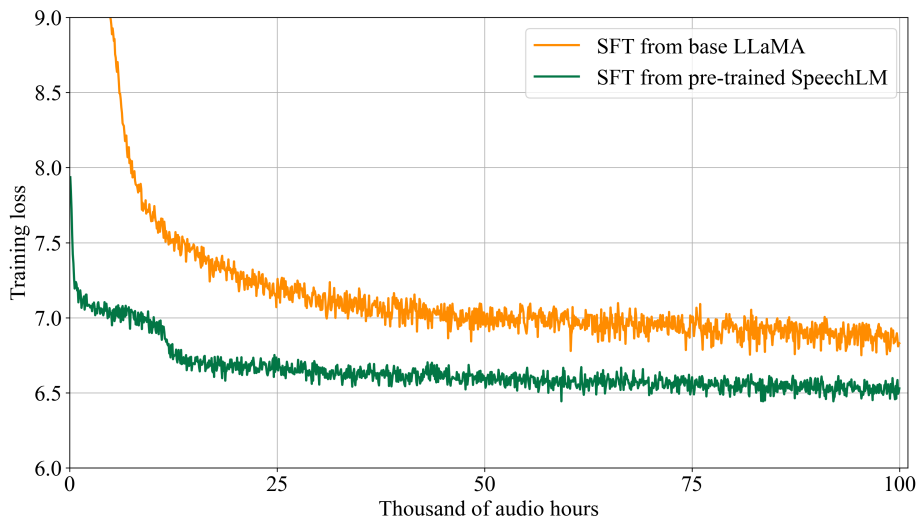


Figure 5. Ablation study on the impact of audio pre-training for SFT of TTS-1. The plot compares SFT loss curves for models initialized from the base LLaMA-3.2-1B checkpoint versus an audio pre-trained version. Both were trained on ~ 100 k audio hours under identical settings.

Additionally, our internal benchmark evaluation shows that pre-training provides substantial improvements in objective metrics: WER improved by approximately 15% and speaker similarity improved by approximately 3% compared to the version without pre-training.

The SFT quality evaluation results are presented in Section 4.

3.5 SpeechLM RL-Alignment

While supervised fine-tuning (SFT) enables the model to generate coherent speech, it inherently optimizes for maximum likelihood estimation on the training data, which may not align with human preferences for speech quality. Speech synthesis presents unique challenges where traditional automatic metrics used in SFT training fail to capture perceptual qualities such as naturalness, expressiveness, and speaker similarity. Moreover, autoregressive speech generation is prone to hallucinations—generating spurious audio tokens that result in artifacts like clicks, pops, or unnatural vocalizations that degrade the listening experience.

Recent advances in text-to-speech research have demonstrated that reinforcement learning (RL) techniques can significantly improve the perceptual quality of synthesized audio [13, 38, 39]. Furthermore, the success of models such as those in the DeepSeek family [40, 18, 41] have established RL as a dominant paradigm in large language model development. Techniques such as Direct Preference Optimization (DPO) [42] and Group Relative Policy Optimization (GRPO) [18] have shown remarkable success in steering model behavior toward human-preferred outcomes, improving both the reliability and usefulness of generated content through iterative feedback mechanisms. Motivated by these developments, we adapt these methodologies to the domain of speech generation, where the primary challenge involves crafting reward signals that effectively capture the complex, subjective aspects of audio quality.

To address these limitations, we employ reinforcement learning (RL) to align the SpeechLM with human preferences for high-quality speech synthesis. Specifically, we use Group Relative Policy Optimization (GRPO) [18], a variant of Proximal Policy Optimization (PPO) that is particularly well-suited for language model alignment tasks.

GRPO formulation. GRPO optimizes the SpeechLM by encouraging it to generate responses that maximize a given reward function while staying close to the original supervised fine-tuned model. It achieves this by updating the model based on an advantage estimate, which measures how much better a generated response is compared to the average response in a batch. To ensure training stability, policy updates are clipped to prevent large deviations from the reference model. Furthermore, a KL divergence penalty is used as a regularization component that constrains the updated policy from diverging excessively from the reference policy, preventing the model from generating degenerate outputs that could arise from unconstrained optimization.

The key innovation in GRPO is the computation of advantages using group-based comparisons rather than individual rewards. For a batch of G responses $\{o_1, \dots, o_G\}$ generated for the same query q , the advantage for response o_i is computed as:

$$\hat{A}_{i,t} = r_i - \text{mean}(\mathbf{r}) \quad (7)$$

where r_i is the reward for response o_i , and $\mathbf{r} = \{r_1, \dots, r_G\}$ is the vector of rewards for all responses in the group. As demonstrated in [43], scaling rewards can introduce a question-level difficulty bias. To address this, we disable reward scaling in GRPO and by default use unscaled, mean-centered advantages for more robust training.

Reward pipeline. To compute the reward signals, each output sequence of audio tokens from the SpeechLM is processed through a multi-stage evaluation pipeline. First, the generated audio token sequences are passed through the audio decoder to reconstruct the corresponding 48 kHz waveforms. These decoded audio samples are then fed into specialized evaluation models to compute the individual reward components: an automatic speech recognition (ASR) model that transcribes the audio to compute WER scores, a speaker verification model extracts embeddings to calculate similarity scores with the reference audio, and a DNSMOS model assesses the perceptual quality of the generated speech. This evaluation pipeline ensures that the reward signals accurately reflect the quality of the final audio output rather than just the token-level predictions.

This group-relative approach reduces variance in advantage estimation and provides more stable training compared to absolute reward-based methods.

Reward function design. Our reward function $R(p, c)$ combines three key components to capture different aspects of speech quality, where p represents the prompt input and c represents the generated completion audio:

$$R(p, c) = \alpha R_{wer}(c) + \beta R_{similarity}(p, c) + \gamma R_{dnsmos}(c) \quad (8)$$

where each component is normalized to the $[0, 1]$ range and addresses specific aspects of speech synthesis quality:

WER reward. R_{wer} represents the word error rate reward, computed by transcribing the generated audio using Whisper-large-v3 model [44] and comparing it against the target text. The raw WER score is normalized using an exponential decay function to map it to the $(0, 1]$ range:

$$R_{wer}(c) = \exp(-k \cdot \text{WER}(c)) \quad (9)$$

where $k = 2.5$ is a scaling parameter that controls the sensitivity to WER values. For languages in the character error rate (CER) evaluation list, character error rate is used instead of word error rate.

Similarity reward. $R_{similarity}$ evaluates speaker similarity between generated and reference audio using deep speaker verification models based on WavLM-large fine-tuned for speaker verification [20]. The cosine similarity score is computed between speaker embeddings and is already in the range $[-1, 1]$, normalized as:

$$R_{similarity}(p, c) = \frac{\text{CosSim}(\text{embed}(p), \text{embed}(c)) + 1}{2} \quad (10)$$

DNSMOS reward. R_{dnsmos} evaluates perceptual speech quality using the Deep Noise Suppression Mean Opinion Score (DNSMOS) [21], whose results are strongly aligned with how humans judge audio quality. The DNSMOS score is already in the range $[1, 5]$ and is normalized as:

$$R_{dnsmos}(c) = \frac{\text{DNSMOS}(c) - 1}{4} \quad (11)$$

The coefficients α, β, γ are hyperparameters that balance the relative importance of each component, with careful tuning required to achieve optimal trade-offs between speech quality, speaker fidelity, and content accuracy. All reward components are designed to be maximized, with higher values indicating better performance.

Extensibility and flexibility. The modular design of our reward function makes it highly extensible for incorporating additional reward signals that capture various aspects of human preferences in TTS perceptual quality. The framework can easily accommodate new reward components by simply extending the linear combination:

$$R(p, c) = \sum_i w_i R_i(p, c) \quad (12)$$

where w_i are the corresponding weights and R_i are individual reward functions.

This flexible architecture allows for rapid experimentation with different reward combinations and enables the incorporation of domain-specific quality metrics tailored to particular applications or user preferences.

Conditional reward activation. An important feature of this framework is the ability to conditionally activate reward signals based on dataset annotations or prompt characteristics. For example, speaking style rewards (e.g., R_{style}) are only applied to samples that contain annotated speaking style tags like [whispering] or [laughing], while emotion consistency rewards ($R_{emotion}$) are activated only for prompts with emotional markup tags such as [angry] or [sad]. Similarly, non-verbal token rewards ($R_{nonverbal}$) are computed only for samples containing non-verbal annotations like [breathe] or [sigh]. This conditional approach ensures that specialized reward signals are applied only to relevant training examples, preventing unnecessary computation and avoiding potential conflicts when evaluating samples that lack the corresponding annotations.

Experiments. We conducted two sets of experiments to evaluate the effectiveness of our GRPO-based RL alignment. Both experiments used the SFT-trained TTS-1 model as the reference policy and were performed on a 1,000-hour subset of our English fine-tuning data. For each prompt, we generated eight responses and computed the rewards for each.

In the first set of experiments, we trained three separate models, each optimized for a single reward signal: WER, speaker similarity, or DNSMOS. In the second experiment, we trained a single model using a combined reward function. For this set of experiments, we weighted WER, speaker similarity, and DNSMOS rewards equally ($\alpha = \beta = \gamma = 1.0$), but it is important to note that these weights can be tuned to prioritize different optimization goals.

Figure 6 shows the training curves for both experimental setups. The left panel demonstrates that each individual reward signal was effective at improving its corresponding metric when trained separately. The right panel shows that the unified approach achieved a strong balance across all three metrics, outperforming the specialized models in overall quality. The combined model demonstrated significant improvements in all three dimensions compared to the SFT baseline, validating our approach of using a composite reward to align the model with multiple facets of human preference for speech quality.

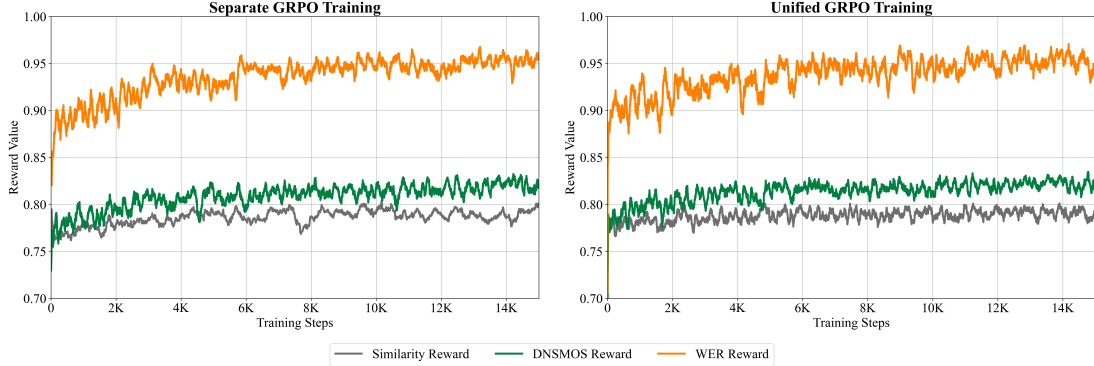


Figure 6. Training curves for GRPO experiments. Left: separate reward signal training, where each model was trained with a single reward (WER, Similarity, or DNSMOS) and evaluated on the corresponding metric. Right: unified model with combined reward function.

3.6 Audio Markups

To facilitate control over speech synthesis prosody and style, independent of the reference audio, we employ embedded text annotations to guide the generation process. These annotations, which we term *audio markups*, are categorized into 8 speaking styles and 7 non-verbal vocalizations, as detailed in Table 5.

Category	Tags
Speaking style	[angry], [disgusted], [fearful], [happy], [laughing], [sad], [surprised], [whispering]
Non-verbals	[breathe], [clear_throat], [cough], [cry], [laugh], [sigh], [yawn]

Table 5. Types of audio markup tags used for conditioning speech synthesis.

Dataset construction. Non-verbal vocalizations are relatively straightforward to incorporate due to their temporally localized nature. The SpeechLM learns to generate these sounds reliably through their direct annotation in the input prompt.

Style control tags present a greater challenge, as the model must maintain high speaker similarity to the reference audio while simultaneously exhibiting the nuanced desired style, which typically corresponds to a specific emotion. This emotion influences the entire utterance, affecting its pace, prosody, tone, and volume.

In initial experiments, wherein individual examples with prepended style control tags were introduced during SFT, we observed that the model failed to utilize these tags, producing no discernible effect on the output. We hypothesized that this failure stems from the audio codec’s design, which encapsulates both acoustic and semantic information within a single latent space. This entanglement prevents the model from isolating the stylistic information from the speaker’s vocal characteristics when tags are simply prepended to the input prompt.

Similar solutions, such as those proposed by [12, 14], use a speaker embedding model to encode the speaker’s voice timbre, thereby explicitly disentangling acoustic and semantic prompting. This design simplifies the training objective, enabling the model to focus on interpreting style tags without the concurrent task of precisely cloning the reference audio but has the drawback of requiring the training of an additional speaker embedding model.

To overcome this, we constructed a dataset by pairing neutral and stylized utterances from the same speaker. For each pair, the corresponding transcripts were concatenated, using the style tag as a delimiter, while the audio files were joined with a 0.5 to 1.5-second silence gap. To augment the data, each neutral utterance was paired with 1 to 5 unique stylized utterances. The dataset also included non-verbal vocalizations, which appeared in $\sim 20\%$ of samples, and retained $\sim 30\%$ of samples as unpaired neutral utterances to preserve fundamental speech synthesis capabilities.

The resulting dataset, composed entirely of English audio and containing approximately 100000 examples, totals 180 hours of audio from 340 unique speakers. A detailed distribution of audio markup tag occurrences is provided in Figure 7.

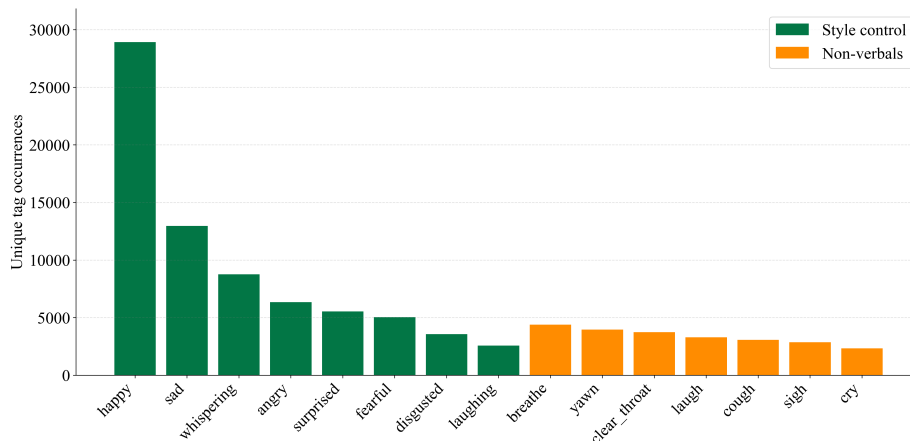


Figure 7. Histogram of occurrences of each audio markup tag.

Experiment setup. A series of ablation studies revealed that both TTS-1 and TTS-1-Max SpeechLMs achieve better generalization, as indicated by lower evaluation loss, when fine-tuned using Low-Rank Adaptation (LoRA) [22] as opposed to full-model SFT. The hyperparameters for LoRA fine-tuning are detailed in Table 6.

Hyperparameter	TTS-1	TTS-1-Max
Per-GPU batch size	4	2
Gradient accumulation steps	1	2
Total number of GPUs	8	
Maximum sequence length	2048	
Optimizer	AdamW, $\beta_1 = 0.9$, $\beta_2 = 0.95$	
Learning rate (peak)	4×10^{-5}	5×10^{-6}
Learning rate schedule	Cosine decay (10% warmup)	
Weight decay	0.1	
LoRA layers	QKVO + MLP	QKVO
LoRA rank	16	
LoRA alpha	32	
LoRA dropout	0.2	

Table 6. Audio markup fine-tuning hyperparameters for TTS-1 and TTS-1-Max.

Evaluation results. The quantitative evaluation of prosodic and non-verbal synthesis fidelity presents a significant challenge. Consequently, we conducted human-based preference testing to assess the model’s controllability via audio markups. These evaluations guided the selection of optimal model checkpoints through a simple voting mechanism. During this process, we noted that the model demonstrated an emergent capability for style generalization to non-English languages, although with reduced fidelity. Furthermore, we observed that combining multiple style tags could produce highly nuanced and intricate vocal performances. Qualitative examples of these phenomena are provided on our project’s demonstration page.

3.7 Infrastructure

This section covers high-level details about the hardware and software setup used for the training and evaluation of the models.

Software. For all the training and evaluations, we use Transformers 4.50.0 [45], PyTorch 2.6.0 [46], CUDA 12.4, and FlashAttention 2.7.4 [32] for SpeechLM training acceleration. For distributed multi-node/multi-GPU training, we use PyTorch Lightning 2.5.0 [47].

Hardware. For SpeechLM pre-training and supervised fine-tuning of both TTS-1 and TTS-1-Max, we used ~ 2 months of 4 NVIDIA H100 GPU nodes (32GPUs total). For audio codec, RL-alignment, audio markup, and all quality evaluations, we used ~ 3 months of 2 NVIDIA A100 GPU nodes (16GPUs total).

Training data storage. To efficiently search training examples, we add indexes stored alongside the audio codes. Even with this overhead, we have achieved a compression ratio of $\sim 500:1$ vs storing raw audio. This significantly reduced storage requirements for training experiments spanning months and utilizing terabytes of distributed storage. Moreover, this reuse of pre-tokenized audio codes for multiple training runs also accelerated the training throughput by alleviating I/O bottlenecks.

4 Quality Evaluation

To evaluate the final performance of Inworld TTS-1 and TTS-1-Max, we generated a benchmark dataset using Gemini 2.5 Pro, comprising 100 sentences for each of the 11 supported languages, for a total of 1100 samples. We then synthesized speech for this dataset using both models with the same set of speakers to ensure a fair comparison. The quality was assessed using the same Word Error Rate (WER) and Speaker Similarity (SIM) metrics described previously.

The results, presented in Figure 8, show that TTS-1-Max consistently outperforms TTS-1 in terms of both WER/CER and SIM across all languages, demonstrating the effectiveness of the larger model in generating more accurate and higher-fidelity speech. Notably, both models achieve very high speaker similarity, indicating their robustness in voice cloning.

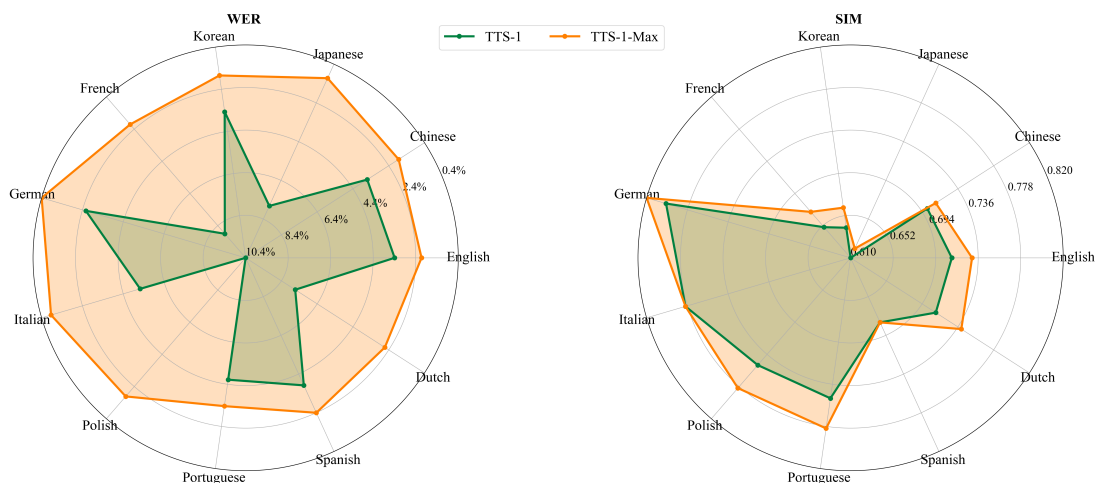


Figure 8. Multilingual evaluation results comparing WER and SIM scores by language. Left: WER (lower is better). Right: SIM (higher is better).

4.1 Evaluation on Varying Input Lengths

To further assess the models’ performance on English, we conducted an evaluation across three datasets with varying input lengths: Short, Medium, and Long. The statistics for these datasets are detailed in Table 7. This evaluation aimed to measure the accuracy and robustness of the models when handling texts of different complexities and durations.

Dataset	Total	Avg Chars	Min Chars	Max Chars
Short	208	7.0	3	12
Medium	150	87.0	41	196
Long	517	153.0	75	225

Table 7. Statistics of English evaluation datasets by input text length.

The evaluation results, shown in Table 8, confirm that TTS-1-Max consistently achieves lower Word Error Rates (WER) across all input lengths compared to TTS-1. This indicates that the larger model is more robust in handling a variety of text lengths, from short phrases to longer sentences. The table also includes the

SFT-only results to demonstrate the improvements achieved through our complete training pipeline including RL alignment.

Model	Short	Medium	Long	Total Avg.
TTS-1 _{SFT}	11.3	4.0	8.5	7.9
TTS-1	9.6	2.3	7.0	6.3
TTS-1-Max _{SFT}	10.1	3.3	7.3	6.9
TTS-1-Max	8.2	1.9	5.2	5.1

Table 8. Word Error Rate (WER) in % on English datasets of varying lengths. Models with _{SFT} subscript show performance after supervised fine-tuning only, while the base models include the complete training pipeline with RL alignment.

4.2 Internal TTS Arena Evaluation

To evaluate our models against commercial TTS systems, we built an internal TTS arena for comparative evaluation. We included five TTS models in our comparison: 11LABS Multilingual V2, Cartesia Sonic 2, OpenAI TTS-1-HD, Inworld TTS-1, and Inworld TTS-1-Max.

The evaluation process involved approximately 20 human annotators conducting blind preference comparisons. The voting process was structured as follows:

1. Randomly select two models from the five-model list.
2. For each model, randomly select the corresponding built-in English speaker.
3. Human annotators enter text to synthesize, generate audio for each pair, and vote for their preferred output.

We collected over 400 votes, and the head-to-head win rates are presented in Table 9. The results show that our Inworld TTS-1-Max model achieved competitive performance, with win rates of 59.1% against 11LABS, 60.9% against Cartesia, 55.3% against Inworld TTS-1, and 60.7% against OpenAI TTS-1-HD. These results demonstrate the effectiveness of our proposed approach in producing high-quality speech that aligns with human preferences.

Model	11labs	Cartesia	OpenAI	Inworld TTS-1	Inworld TTS-1-Max
11labs	-	64.3% (27/42)	48.9% (22/45)	44.0% (22/50)	40.9% (18/44)
Cartesia	35.7% (15/42)	-	40.4% (21/52)	36.8% (14/38)	39.1% (18/46)
OpenAI	51.1% (23/45)	59.6% (31/52)	-	43.9% (18/41)	39.3% (11/28)
Inworld TTS-1	56.0% (28/50)	63.2% (24/38)	56.1% (23/41)	-	44.7% (21/47)
Inworld TTS-1-Max	59.1% (26/44)	60.9% (28/46)	60.7% (17/28)	55.3% (26/47)	-

Table 9. Head-to-head win rates from internal TTS arena evaluation. Each cell shows the win rate of the row model against the column model, with the number of wins and total comparisons in parentheses.

5 Inference

Inworld TTS-1 and TTS-1-Max alike support 2 modes of execution:

- **Instant voice cloning** - the model uses only the reference audio and its transcript to produce new generations.
- **Professional voice cloning** - the model’s SpeechLM is LoRA fine-tuned on the given user’s voices recordings to further enhance similarity to the reference speaker.

Both execution modes can operate within our streaming inference pipeline, which is designed for real-time speech synthesis. The pipeline generates streaming audio segments through a careful orchestration of the SpeechLM and audio decoder. The process begins with the SpeechLM autoregressively generating audio tokens, which accumulate in a buffer. Once a buffer of a specified size is formed, the audio decoder converts this tokenized representation into 48 kHz waveform segments for delivery to the user. The following sections detail the solutions we engineered in pursuit of optimized responsiveness.

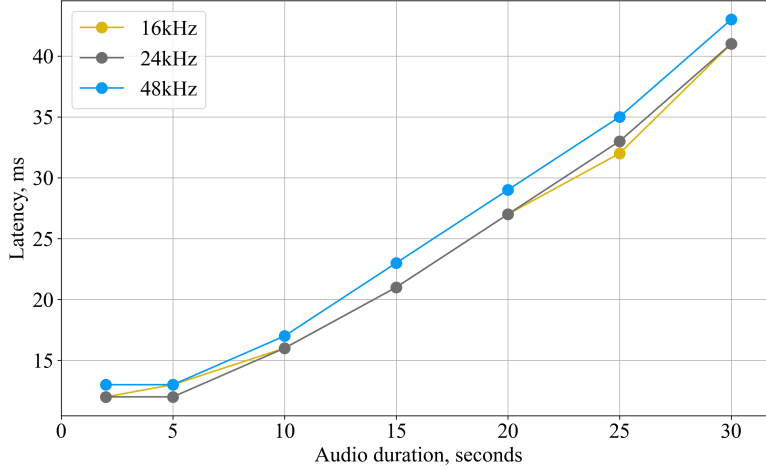


Figure 9. Audio decoder latency comparison across different sample rates and audio durations.

5.1 Decoder

While streaming support helped to reduce the time to get the first audio chunk, it also introduced new challenges for the decoder. Specifically, the decoder must generate audio waveforms in a manner that transitions smoothly during concatenation. We observed that artifacts emerge when trying to concatenate audio segments with slight discontinuities [15], and the inconsistency in the volume of the generated audio segments can lead to a noticeable drop in the quality of the speech. We combine the following techniques to address these issues.

Concatenation at the non-voicing regions. To mitigate the artifacts caused by the audio discontinuity [15], we propose a simple yet effective voice streaming method that only allows the audio segments to be concatenated at the non-voicing regions (e.g., a short silence between the words). When a new audio segment $\hat{X}_{t_1:t_2}$ is decoded, with t_1 and t_2 being the start and end time of the segment, we search for the last fixed-radius non-voicing region $\hat{X}_{t^*-\Delta t:t^*+\Delta t}$ that satisfies

$$\max |\hat{X}_{t^*-\Delta t:t^*+\Delta t}| < \epsilon, \quad (13)$$

where Δt is the radius of the non-voicing region, and ϵ is the threshold for the signal magnitude. If such a non-voicing region exists, the decoded audio waveform up to t^* is emitted to the output stream, then the remaining audio waveform $\hat{X}_{t^*:t_2}$ is discarded. The tokens that correspond to the discarded audio are retained and will be processed in the next chunk. Similarly, if no region that satisfies Equation 13 is found, we discard the entire segment $\hat{X}_{t_1:t_2}$, deferring all the audio tokens for subsequent processing.

Volume stabilization. Based on the observation of increased volume inconsistency in short audio segments, we propose to stabilize the volume of the generated audio by extending the context of the audio decoder. Specifically, to generate audio segment $\hat{X}_{t_1:t_2}$, we feed the audio decoder with tokens that correspond to $\hat{X}_{t_1-\Delta T:t_2}$, where ΔT is a fixed-length context. Then we remove $\hat{X}_{t_1-\Delta T:t_1}$ to obtain the desired output. Given the fact (in Table. 9) that audio decoding is much faster than audio token generation, this method removes audible volume inconsistency with negligible latency overhead.

Decoding the prompt audio. We also observed that extending the context of the audio decoder to include the prompt audio can further improve the model’s ability to replicate speaker identity. Results in Table. 10 show that, in the non-streaming setting, the similarity scores between the prompt and the generated audio are higher if the decoder is fed with the concatenation of both the prompt audio tokens and the generated audio tokens. In the streaming setting, this approach also benefits initial segments of the generated audio, through the extended context of the audio decoder.

Setting	SIM
Decode without prompt	0.495
Decode with prompt	0.535

Table 10. Speaker similarity comparison between the audio prompt and the generated audio in the non-streaming setting. Results are computed on the English subset of the Seed-TTS evaluation [13].

5.2 Architecture Optimizations

To further improve latency, we collaborated with the Modular team to optimize the inference engine, resulting in several key architectural and kernel-level improvements.

- The serving pipeline employs a multi-step scheduler for asynchronous speech token generation, allowing the SpeechLM to produce a batch of tokens entirely on the GPU without CPU interruption, which significantly enhances GPU utilization.
- The audio decoder was re-architected to support batched inputs with padding, using custom kernels to ensure correct output and process multiple sequences simultaneously.
- For high-performance penalty sampling, token occurrence metadata is stored in a sparse format to avoid the overhead of large tensors. The entire penalty and sampling process is executed on the GPU through highly optimized kernels written in the Mojo programming language.
- The inference stack leverages a graph compiler (MAX pipeline) for optimizations like kernel fusion and memory planning, complemented by custom kernels for critical operations like attention and matrix-vector multiplication, which were also developed in Mojo to outperform standard library implementations.

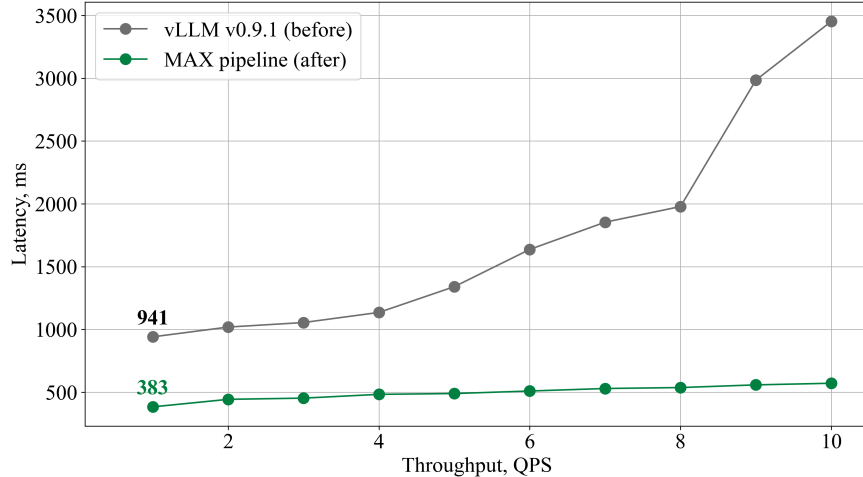


Figure 10. P90 latency comparison for the first 2-second audio chunk between the vanilla vLLM solution and the Modular-optimized implementation.

As a result of these combined optimizations, the streaming API delivers the first two seconds of synthesized audio on average 70% faster than a vanilla vLLM-based implementation [48], as shown in Figure 10.

5.3 Model Constraints and Trade-Offs

While the proposed inference architecture is highly efficient, it has several inherent limitations.

A key optimization is caching reference prompt audio tokens to improve latency. However, this can cause emotional and stylistic characteristics to bleed from the reference audio into the generated speech, making it difficult to disentangle speaker identity from the reference prosody.

Furthermore, the duration of the reference audio constrains the maximum length of reliable output; longer sequences generated from short prompts may suffer from quality degradation.

The autoregressive nature of the SpeechLM necessitates a trade-off in decoding parameters. For example, a lower sampling temperature can improve speaker similarity but reduce expressiveness. As a result, inference parameters must be tuned for specific use cases.

Finally, imbalances in the training data affect generalization, leading to varied quality across languages and inconsistent effectiveness of audio markup tags.

6 Ethical Considerations and Safeguards

The development of powerful generative models for speech synthesis, particularly those with zero-shot voice cloning capabilities, raises important ethical considerations. The potential for misuse of such technology, such as the creation of synthetic media for malicious purposes, requires a proactive approach to safety. Accordingly, we have chosen not to publicly release the model weights to mitigate these risks.

In addition, all audio generated for production applications is integrated with an inaudible watermark. This technique provides a mechanism for content authentication and helps in distinguishing synthetic speech from human speech, further addressing concerns about potential misuse.

As an additional safeguard, users must explicitly confirm they have the rights to any voice they intend to clone using the instant voice cloning feature in the Inworld TTS Portal.

7 Conclusion

In this paper, we introduced Inworld TTS-1 and TTS-1-Max, two LLM-based text-to-speech models that demonstrate exceptional quality, controllability, and multilingual support. Our three-stage training process combining large-scale pre-training, supervised fine-tuning, and reinforcement learning alignment has proven effective in developing high-performance TTS systems. The development of a novel high-resolution audio codec and careful instruction data curation are key contributions that enable the generation of 48 kHz speech with fine-grained control over emotion and non-verbal vocalizations.

Despite this significant progress, our work also highlights several areas for future improvement. We believe that more thorough and systematic data preparation and cleaning are crucial for pushing the boundaries of speech synthesis quality. While our filtering pipeline was effective, developing more sophisticated data curation techniques could lead to even cleaner and more diverse training sets, further reducing synthesis artifacts and improving overall naturalness.

Furthermore, our evaluations, while comprehensive, reveal limitations in capturing the nuances of real-world performance. For instance, we observed that metrics like speaker similarity can fluctuate with emotionally expressive speech delivery, suggesting that current automated evaluation protocols may not fully capture perceptual quality in dynamic, real-world scenarios. Future work should focus on developing more robust evaluation methodologies that better account for prosodic and emotional variations, bridging the gap between quantitative metrics and human perception.

By open-sourcing our training, modeling, and benchmarking code, we hope to encourage the community to build upon our work, address these challenges, and contribute to the development of more robust, expressive, and natural-sounding speech synthesis technologies.

Credit Attribution and Acknowledgements

Please cite this work as "Inworld AI (2025)".

Training Infrastructure

Compute cluster setup

Igor Poletaev, Zhifeng Deng

Distributed training implementation

Igor Poletaev, Yufei Feng, Feifan Fan, Phillip Dang

Training speed optimizations

Igor Poletaev

Audio Codec

Audio data collection

Yufei Feng, Igor Poletaev

Training pipeline implementation

Yufei Feng

Training run babysitting

Yufei Feng

Pre-Training

Audio data collection

Phillip Dang, Igor Poletaev

Text data collection

Igor Poletaev

Training pipeline implementation

Igor Poletaev

Training run babysitting

Igor Poletaev

Fine-Tuning

Audio data collection

Igor Poletaev, Pavel Filimonov, Phillip Dang, Yufei Feng, Feifan Fan, Michael Ermolenko

Data annotation and filtering

Igor Poletaev, Pavel Filimonov, Phillip Dang, Yufei Feng, Feifan Fan, Michael Ermolenko, Mikhail Karpik

Optimizations and architecture

Igor Poletaev, Yufei Feng, Michael Ermolenko

Training runs babysitting

Igor Poletaev

RL Alignment

Audio data collection

Feifan Fan, Igor Poletaev

Data annotation and filtering

Feifan Fan, Igor Poletaev

Training pipeline implementation

Feifan Fan

Training runs babysitting

Feifan Fan

Quality Evaluations

Benchmarking data collection

Feifan Fan, Igor Poletaev

Benchmarking infrastructure

Feifan Fan, Igor Poletaev, Phillip Dang, Yufei Feng

Production Serving

Compute cluster setup

Zhifeng Deng, Oleg Atamanenko, Nurullah Morshed

Deployment

Zhifeng Deng, Pavel Karpik, Feifan Fan, Oleg Atamanenko, Nurullah Morshed

Architecture optimizations

Pavel Karpik, (Tyler Kenney, Brian Zhang, Austin Doolittle, Shouzheng Liu, Hengjie Wang, Chris Elrod)¹

Text pre-processing and normalization

Pavel Filimonov, Pavel Karpik

Audio post-processing

Yufei Feng, Pavel Karpik

Prebuilt voice selection

Robert Villahermosa, Jean Wang, Phillip Dang, Igor Poletaev

Quality assurance

Anna Chalova, Robert Villahermosa, Jean Wang, Phillip Dang

Audio watermarking

Pavel Karpik

Voice cloning infrastructure

Jimmy Du, Vikram Sivaraja, Rinat Takhautdinov, Peter Skirko, Oleg Atamanenko, Mikhail Mamontov, Feifan Fan

Inworld TTS Portal UI & UX

Jasmine Mai, Dmytro Semernia, Joseph Coombes, Jean Wang, Suri Mao, Valeria Gusarova

Public API

Ian Lee, Jimmy Du, Pavel Karpik, Igor Poletaev

Additional Contributions

Blog post & paper content

Igor Poletaev, Feifan Fan, Yufei Feng, Evgenii Shingarev, Joseph Coombes

Launch partners

Cheryl Fichter, Nikki Cope, Louis Fischer

Legal

Oliver Louie

System administration & on-call support

Oleg Atamanenko, Nurullah Morshed, Evgenii Shingarev

Communications

Kylan Gibbs, Florin Radu, Cheryl Fichter, Andreas Assad Kottner

Technical report

Igor Poletaev, Feifan Fan, Yufei Feng, Phillip Dang, Pavel Karpik

Authorship & credit attribution

Igor Poletaev

We thank all Inworld AI team members for their contributions, including those not explicitly named above. These results would not have been possible without our collective effort.

We also thank our partners: Oracle and the OCI HPC team for infrastructure support, Voltage Park for providing H100 GPUs, and the amazing Modular team for optimizing model serving and making its real-time inference ready.

¹Modular Team

References

- [1] Daniel Galvez, Greg Diamos, Juan Ciro, Juan Felipe Cerón, Keith Achorn, Anjali Gopi, David Kanter, Maximilian Lam, Mark Mazumder, and Vijay Janapa Reddi. The people’s speech: A large-scale diverse english speech recognition dataset for commercial usage. *arXiv preprint arXiv:2111.09344*, 2021.
- [2] Xinjian Li, Shinnosuke Takamichi, Takaaki Saeki, William Chen, Sayaka Shiota, and Shinji Watanabe. Yodas: Youtube-oriented dataset for audio and speech. pages 1–8, 2023.
- [3] Haorui He, Zengqiang Shang, Chaoren Wang, Xuyuan Li, Yicheng Gu, Hua Hua, Liwei Liu, Chen Yang, Jiaqi Li, Peiyang Shi, et al. Emilia: An extensive, multilingual, and diverse speech dataset for large-scale speech generation. pages 885–890, 2024.
- [4] Yinghao Aaron Li, Cong Han, Vinay Raghavan, Gavin Mischler, and Nima Mesgarani. Styletts 2: Towards human-level text-to-speech through style diffusion and adversarial training with large speech language models. *Advances in Neural Information Processing Systems*, 36:19594–19621, 2023.
- [5] Yi Ren, Yangjun Ruan, Xu Tan, Tao Qin, Sheng Zhao, Zhou Zhao, and Tie-Yan Liu. FastSpeech: Fast, robust and controllable text to speech. *Advances in neural information processing systems*, 32, 2019.
- [6] James Betker. Better speech synthesis through scaling. *arXiv preprint arXiv:2305.07243*, 2023.
- [7] Jaehyeon Kim, Jungil Kong, and Juhee Son. Conditional variational autoencoder with adversarial learning for end-to-end text-to-speech. pages 5530–5540, 2021.
- [8] Matthew Le, Apoorv Vyas, Bowen Shi, Brian Karrer, Leda Sari, Rashel Moritz, Mary Williamson, Vimal Manohar, Yossi Adi, Jay Mahadeokar, et al. Voicebox: Text-guided multilingual universal speech generation at scale. *Advances in neural information processing systems*, 36:14005–14034, 2023.
- [9] Alec Radford, Jeffrey Wu, Rewon Child, David Luan, Dario Amodei, Ilya Sutskever, et al. Language models are unsupervised multitask learners. *OpenAI blog*, 1(8):9, 2019.
- [10] Jordan Hoffmann, Sebastian Borgeaud, Arthur Mensch, Elena Buchatskaya, Trevor Cai, Eliza Rutherford, Diego de Las Casas, Lisa Anne Hendricks, Johannes Welbl, Aidan Clark, et al. Training compute-optimal large language models. *arXiv preprint arXiv:2203.15556*, 2022.
- [11] Chengyi Wang, Sanyuan Chen, Yu Wu, Ziqiang Zhang, Long Zhou, Shujie Liu, Zhuo Chen, Yanqing Liu, Huaming Wang, Jinyu Li, et al. Neural codec language models are zero-shot text to speech synthesizers. *arXiv preprint arXiv:2301.02111*, 2023.
- [12] Bowen Zhang, Congchao Guo, Geng Yang, Hang Yu, Haozhe Zhang, Heidi Lei, Jialong Mai, Junjie Yan, Kaiyue Yang, Mingqi Yang, et al. Minimax-speech: Intrinsic zero-shot text-to-speech with a learnable speaker encoder. *arXiv preprint arXiv:2505.07916*, 2025.
- [13] Philip Anastassiou, Jiawei Chen, Jitong Chen, Yuanzhe Chen, Zhuo Chen, Ziyi Chen, Jian Cong, Lelai Deng, Chuang Ding, Lu Gao, et al. Seed-tts: A family of high-quality versatile speech generation models. *arXiv preprint arXiv:2406.02430*, 2024.
- [14] Zhihao Du, Qian Chen, Shiliang Zhang, Kai Hu, Heng Lu, Yexin Yang, Hangrui Hu, Siqi Zheng, Yue Gu, Ziyang Ma, et al. Cosyvoice: A scalable multilingual zero-shot text-to-speech synthesizer based on supervised semantic tokens. *arXiv preprint arXiv:2407.05407*, 2024.
- [15] Zhihao Du, Yuxuan Wang, Qian Chen, Xian Shi, Xiang Lv, Tianyu Zhao, Zhifu Gao, Yexin Yang, Changfeng Gao, Hui Wang, et al. Cosyvoice 2: Scalable streaming speech synthesis with large language models. *arXiv preprint arXiv:2412.10117*, 2024.
- [16] Maurice Weber, Dan Fu, Quentin Anthony, Yonatan Oren, Shane Adams, Anton Alexandrov, Xiaozhong Lyu, Huu Nguyen, Xiaozhe Yao, Virginia Adams, et al. Redpajama: an open dataset for training large language models. *Advances in neural information processing systems*, 37:116462–116492, 2024.
- [17] LAION. Open instruction generalist (oig) dataset. <https://laion.ai/blog/oig-dataset/>, 2023.
- [18] Zhihong Shao, Peiyi Wang, Qihao Zhu, Runxin Xu, Junxiao Song, Xiao Bi, Haowei Zhang, Mingchuan Zhang, YK Li, Y Wu, et al. Deepseekmath: Pushing the limits of mathematical reasoning in open language models, 2024. URL <https://arxiv.org/abs/2402.03300>.

- [19] Zhen Ye, Xinfu Zhu, Chi-Min Chan, Xinsheng Wang, Xu Tan, Jiahe Lei, Yi Peng, Haohe Liu, Yizhu Jin, Zheqi DAI, et al. Llasa: Scaling train-time and inference-time compute for llama-based speech synthesis. *arXiv preprint arXiv:2502.04128*, 2025.
- [20] Sanyuan Chen, Chengyi Wang, Zhengyang Chen, Yu Wu, Shujie Liu, Zhuo Chen, Jinyu Li, Naoyuki Kanda, Takuya Yoshioka, Xiong Xiao, et al. Wavlm: Large-scale self-supervised pre-training for full stack speech processing. *IEEE Journal of Selected Topics in Signal Processing*, 16(6):1505–1518, 2022.
- [21] Chandan KA Reddy, Vishak Gopal, and Ross Cutler. Dnsmos p. 835: A non-intrusive perceptual objective speech quality metric to evaluate noise suppressors. In *ICASSP 2022-2022 IEEE international conference on acoustics, speech and signal processing (ICASSP)*, pages 886–890. IEEE, 2022.
- [22] Edward J Hu, Yelong Shen, Phillip Wallis, Zeyuan Allen-Zhu, Yuanzhi Li, Shean Wang, Lu Wang, Weizhu Chen, et al. Lora: Low-rank adaptation of large language models. *ICLR*, 1(2):3, 2022.
- [23] Kaiming He, Xiangyu Zhang, Shaoqing Ren, and Jian Sun. Deep residual learning for image recognition. In *Proceedings of the IEEE conference on computer vision and pattern recognition*, pages 770–778, 2016.
- [24] Aaron Grattafiori, Abhimanyu Dubey, Abhinav Jauhri, Abhinav Pandey, Abhishek Kadian, Ahmad Al-Dahle, Aiesha Letman, Akhil Mathur, Alan Schelten, Alex Vaughan, et al. The llama 3 herd of models. *arXiv preprint arXiv:2407.21783*, 2024.
- [25] NVIDIA Corporation. Matrix multiplication background user’s guide. <https://docs.nvidia.com/deeplearning/performance/dl-performance-matrix-multiplication/index.html#requirements-tc>, 2023.
- [26] John Hewitt. Initializing new word embeddings for pretrained language models. <https://nlp.stanford.edu/~johnhew/vocab-expansion.html>, 2021.
- [27] Detai Xin, Xu Tan, Shinnosuke Takamichi, and Hiroshi Saruwatari. Bigcodec: Pushing the limits of low-bitrate neural speech codec. *arXiv preprint arXiv:2409.05377*, 2024.
- [28] Jungil Kong, Jaehyeon Kim, and Jaekyoung Bae. Hifi-gan: Generative adversarial networks for efficient and high fidelity speech synthesis. *Advances in neural information processing systems*, 33:17022–17033, 2020.
- [29] Alexandre Défossez, Jade Copet, Gabriel Synnaeve, and Yossi Adi. High fidelity neural audio compression. *arXiv preprint arXiv:2210.13438*, 2022.
- [30] Shrimai Prabhumoye, Mostofa Patwary, Mohammad Shoeybi, and Bryan Catanzaro. Adding instructions during pretraining: Effective way of controlling toxicity in language models. *arXiv preprint arXiv:2302.07388*, 2023.
- [31] Yoshua Bengio, Réjean Ducharme, Pascal Vincent, and Christian Jauvin. A neural probabilistic language model. *Journal of machine learning research*, 3(Feb):1137–1155, 2003.
- [32] Tri Dao. Flashattention-2: Faster attention with better parallelism and work partitioning. *arXiv preprint arXiv:2307.08691*, 2023.
- [33] Diederik P Kingma. Adam: A method for stochastic optimization. *arXiv preprint arXiv:1412.6980*, 2014.
- [34] Shen Li, Yanli Zhao, Rohan Varma, Omkar Salpekar, Pieter Noordhuis, Teng Li, Adam Paszke, Jeff Smith, Brian Vaughan, Pritam Damania, et al. Pytorch distributed: Experiences on accelerating data parallel training. *arXiv preprint arXiv:2006.15704*, 2020.
- [35] Yanli Zhao, Andrew Gu, Rohan Varma, Liang Luo, Chien-Chin Huang, Min Xu, Less Wright, Hamid Shojanazeri, Myle Ott, Sam Shleifer, et al. Pytorch fsdp: experiences on scaling fully sharded data parallel. *arXiv preprint arXiv:2304.11277*, 2023.
- [36] Lacombe Yoach, Vaibhav Srivastav, and Sanchit Gandhi. Parler-tts. <https://github.com/huggingface/parler-tts>, 2024.
- [37] Samyam Rajbhandari, Jeff Rasley, Olatunji Ruwase, and Yuxiong He. Zero: Memory optimizations toward training trillion parameter models. In *SC20: International Conference for High Performance Computing, Networking, Storage and Analysis*, pages 1–16. IEEE, 2020.

- [38] Zhihao Du, Changfeng Gao, Yuxuan Wang, Fan Yu, Tianyu Zhao, Hao Wang, Xiang Lv, Hui Wang, Chongjia Ni, Xian Shi, et al. Cosyvoice 3: Towards in-the-wild speech generation via scaling-up and post-training. *arXiv preprint arXiv:2505.17589*, 2025.
- [39] Chen Chen, Yuchen Hu, Wen Wu, Helin Wang, Eng Siong Chng, and Chao Zhang. Enhancing zero-shot text-to-speech synthesis with human feedback. *arXiv preprint arXiv:2406.00654*, 2024.
- [40] Aixin Liu, Bei Feng, Bing Xue, Bingxuan Wang, Bochao Wu, Chengda Lu, Chenggang Zhao, Chengqi Deng, Chenyu Zhang, Chong Ruan, et al. Deepseek-v3 technical report. *arXiv preprint arXiv:2412.19437*, 2024.
- [41] Xiao Bi, Deli Chen, Guanting Chen, Shanhuang Chen, Damai Dai, Chengqi Deng, Honghui Ding, Kai Dong, Qiusi Du, Zhe Fu, et al. Deepseek llm: Scaling open-source language models with longtermism. *arXiv preprint arXiv:2401.02954*, 2024.
- [42] Rafael Rafailov, Archit Sharma, Eric Mitchell, Christopher D Manning, Stefano Ermon, and Chelsea Finn. Direct preference optimization: Your language model is secretly a reward model. *Advances in neural information processing systems*, 36:53728–53741, 2023.
- [43] Zichen Liu, Changyu Chen, Wenjun Li, Penghui Qi, Tianyu Pang, Chao Du, Wee Sun Lee, and Min Lin. Understanding rl-zero-like training: A critical perspective. *arXiv preprint arXiv:2503.20783*, 2025.
- [44] Alec Radford, Jong Wook Kim, Tao Xu, Greg Brockman, Christine McLeavey, and Ilya Sutskever. Robust speech recognition via large-scale weak supervision. In *International conference on machine learning*, pages 28492–28518. PMLR, 2023.
- [45] Thomas Wolf, Lysandre Debut, Victor Sanh, Julien Chaumond, Clement Delangue, Anthony Moi, Pierric Cistac, Tim Rault, Rémi Louf, Morgan Funtowicz, et al. Huggingface’s transformers: State-of-the-art natural language processing. *arXiv preprint arXiv:1910.03771*, 2019.
- [46] A Paszke. Pytorch: An imperative style, high-performance deep learning library. *arXiv preprint arXiv:1912.01703*, 2019.
- [47] William A Falcon. Pytorch lightning. <https://github.com/PyTorchLightning/pytorch-lightning>, 2019.
- [48] Woosuk Kwon, Zhuohan Li, Siyuan Zhuang, Ying Sheng, Lianmin Zheng, Cody Hao Yu, Joseph Gonzalez, Hao Zhang, and Ion Stoica. Efficient memory management for large language model serving with pagedattention. pages 611–626, 2023.